# Assessing Photoreceptor Structure in Macular Hole using Split-detector Adaptive Optics Scanning Light Ophthalmoscopy

Edward L Randerson,[1] Drew Davis,[2] Brian Higgins,[3] Judy E Kim,[4] Dennis P Han,[4] Thomas B Connor,[5] William J Wirostko[5] and Joseph Carroll[4]

*1. Medical Student; 2. Ophthalmology Resident; 3. Research Technologist; 4. Professor of Ophthalmology; 5. Associate Professor of Ophthalmology, Medical College of Wisconsin, Department of Ophthalmology, Milwaukee, Wisconsin, US*

## Abstract

**Introduction:** Macular hole (MH) and vitreomacular traction (VMT) can involve disruption at the level of the photoreceptor interdigitation zone (IZ) and ellipsoid zone (EZ) with optical coherence tomography (OCT). Confocal adaptive optics scanning light ophthalmoscopy (AOSLO) has been used to examine the photoreceptor mosaic following surgical intervention in patients with MH and VMT, showing large 'dark areas' devoid of normal waveguiding cones. Using split-detector AOSLO, which allows visualisation of cone photoreceptor inner segments, we examined the macular cone structure in these disruptions. **Methods:** Seven eyes from six subjects with MH or VMT were imaged with spectral domain OCT (SD-OCT), confocal AOSLO and non-confocal split-detection AOSLO following pars plana vitrectomy (PPV) for MH or intravitreal injection with ocriplasmin for VMT. **Results:** Split-detector AOSLO imagery revealed remnant inner segment structure within dark areas observed with confocal AOSLO. In addition, split-detector images demonstrated that not all hyperreflective dots in confocal AOSLO images were derived from cones. **Conclusion:** Split-detector AOSLO provides additional information for these retinal conditions, and is likely to become an invaluable tool for assessing residual cone structure in conditions where disrupted cone structure interferes with the ability to visualise cells with confocal AOSLO.

## Keywords

Adaptive optics, macular hole, vitreomacular traction, optical coherence tomography, photoreceptor, inner segment

**Disclosure**: Edward L Randerson, Drew Davis, Brian Higgins, Judy E Kim, Dennis P Han, Thomas B Connor, William J Wirostko and Joseph Carroll have no conflicts of interest to declare. No funding was received in the publication of this article. The authors wish to thank Kainat Akhter, Rob Cooper, Mara Goldberg, Moataz Razeen, Chris Skumatz, Melissa Wilk and Jon Young for assistance with retinal imaging.



**Compliance with Ethics Guidelines**: All procedures were followed in accordance with the responsible committee on human experimentation and with the Helsinki Declaration of 1975 and subsequent revisions. Informed consent was received from the all patients involved in the study.

**Received**: 5 May 2015 **Accepted**: 30 June 2015 **Citation**: *European Ophthalmic Review*, 2015;9(1):59–63 *DOI: 10.17925/EOR.2015.09.01.59*

**Correspondence**: Joseph Carroll, The Eye Institute, 925 N 87th St Milwaukee, WI, US. E: jcarroll@mcw.edu

**Support**: Supported by National Institutes of Health (NIH) grant P30EY001931, Thomas M Aaberg, Sr, Retina Research Fund, Foundation Fighting Blindness, RD and Linda Peters Foundation and an unrestricted departmental grant from Research to Prevent Blindness, Inc., New York, NY. This investigation was conducted in a facility constructed with support from the Research Facilities Improvement Program, Grant Number C06RR016511, from the National Center for Research Resources, National Institutes of Health. The sponsors or funding organisations had no role in the design or conduct of this research.

Macular hole (MH) and vitreomacular traction (VMT) can result in disruption of the vital area of contact between the photoreceptors and the nourishing retinal pigment epithelium (RPE).[1–3] Optical coherence tomography (OCT) has become the gold standard tool for diagnosing and managing these conditions.[3–5] OCT is often used for monitoring surgical outcomes in patients with MH and VMT, to ensure that the hole has closed or VMT has released. However, in some patients, despite achieving the desired anatomical outcome, disruptions are seen at the level of the photoreceptor bands on OCT (EZ and IZ). In other patients, despite less-than-expected visual improvement, no abnormality is seen on OCT. In fact, there are inconsistencies across studies comparing OCT findings to visual acuity.[5–13] While the integrity of the photoreceptors is of greatest interest in both, the limited lateral resolution of OCT precludes quantitative assessment of photoreceptors by enumeration and cellular integrity. Given that photoreceptor structure may hold prognostic value for patients with MH and VMT after surgical intervention, there is a requirement to develop advanced imaging approaches in these patients. Adaptive optics scanning light ophthalmoscopy (AOSLO) is capable of correcting the eye's monochromatic aberrations, enabling *in vivo* imaging of the photoreceptor mosaic with cellular resolution.[14,15] AOSLO has been used to image patients with EZ/IZ abnormalities due to ocular trauma,[16] following surgical closure of idiopathic MH[17–19] and eyes with epiretinal membrane (ERM).[20] A general finding in previous patients was the consistent presence of 'dark areas' within the central macula; previously, it had been suggested that these areas were due to cone cell loss.[17,19] However, conventional confocal AOSLO suffers from a significant limitation – detection of photoreceptor cells relies on proper waveguiding of light by structurally intact cells.[21] Thus, loss of the reflective signal on confocal AOSLO in these patients may be due to damaged as opposed to absent cone cells. Resolving this matter is critical to realising the full potential of advanced imaging for evaluating surgical outcomes and establishing realistic expectations

**Table 1: Subject Data**

| Subject Number (Sex/Age) | Eye Imaged | Diagnosis with SD-OCT | Pre-intervention BCVA | Time Post Intervention (days) | Pre-imaging BCVA | Lens Status |
|---|---|---|---|---|---|---|
| PK_0858 (M/60) | OD | MH | 20/40 | 926 | 20/20 (-1) | Pseudophakic† |
| JK_10190 (F/76) | OS | MH | 20/100 | 352 | 20/25 (+0) | Pseudophakic |
| JK_10189 (F/58) | OS | MH | 20/200 | 267 | 20/63 (+3) | Pseudophakic |
| DH_10244 (F/60) | OD | MH | 20/70 | 105 | 20/63 (+2) | Phakic |
| DH_10330 (M/69) | OD | MH | 20/60 | 55 | 20/40 (-1) | Pseudophakic† |
| TC_10209 (F/64) | OD | VMT | 20/70 | 391 | 20/50 (+2) | Phakic |
| TC_10209 (F/64) | OS | VMT | 20/50 | 9 | 20/40 (+3) | Phakic |

*†Subject was fitted with a posterior chamber intraocular lens (PCIOL). BCVA = best-corrected visual acuity; F = female; M = male; MH = macular hole; OD = right eye; OS = left eye; SD-OCT = spectral domain optical coherence tomography; VMT = vitreomacular traction.*

for patients. Recently, a non-confocal technique called 'split-detector' AOSLO was developed, which detects multiply scattered light from the photoreceptor inner segments.[21] This permits visualisation of cones in a manner that appears to be independent of their ability to waveguide light. It has been shown, in various patient populations, that areas appearing dark on confocal AOSLO can still retain an intact inner segment structure.[18,21] Here we used split-detector AOSLO to examine dark areas observed on confocal AOSLO in patients following surgical intervention for MH or VMT, with the goal to more accurately characterise the status of residual cone structure in these patients. We found that dark areas within confocal AOSLO imagery often contain remnant cone inner segment structure. The degree to which these cones are functional remains unclear, but the imaging approach used here provides an important tool for examining the structure–function relationship in MH, VMT and related conditions.

## Methods

### Human Subjects

This research followed the tenets of the Declaration of Helsinki and was approved by the Institutional Review Board at the Medical College of Wisconsin. Informed consent was obtained and documented for all subjects prior to imaging. Six subjects (two male; four female) with MH and VMT lesions participated in spectral domain optical coherence tomography (SD-OCT) and AOSLO imaging. Seven eyes, five with MH and two with VMT, were included in this study. The age (average = 66 years), time post-intervention, pre-intervention best-corrected visual acuity (BCVA), pre-imaging BCVA and lens status varied between subjects (see *Table 1*). Axial length was measured in all eyes using an intraocular lens (IOL) Master (Carl Zeiss Meditec, Dublin, CA, US) to facilitate accurate lateral scaling of retinal images.

### Spectral Domain Optical Coherence Tomography

Images were obtained using SD-OCT (Bioptigen, Inc., Durham, NC, US) just prior to AOSLO imaging. Linear B-scans (1,000 A-scans/B-scan; 100 repeated B-scans) were averaged as previously described.[22] In addition 3 x 3 mm (1,000 A-scans/B-scan; 400 B-scans/volume) and/or 7 x 7 mm (1,000 A-scans/B-scan; 250 B-scans/volume) volumetric scans were acquired from each eye.

### Adaptive Optics Scanning Light Ophthalmoscopy

AOSLO imaging included simultaneous collection of images using both confocal and split-detection channels. Full system details have been previously described.[14,21] A 790 nm superluminescent diode was used for imaging, with the field of view of each image subtending either 1 x 1° or 1.5 x 1.5°. An internal fixation target was used to guide fixation and allow acquisition of images from different retinal locations. Individual image sequences at each fixation location contained 150 frames. Each image sequence was 'desinusoided' to correct distortions introduced by the sinusoidal movement of the resonant scanner. Next, a reference frame within each image sequence having minimal distortion and maximal sharpness was identified, and registration of frames within a given image sequence to their respective reference frame was performed using a previously described strip-registration algorithm (Python; Python Software Foundation).[23] A final image for each image sequence was created by averaging together the frames with the highest normalised cross-correlation to the reference frame. The split-detector images were processed in parallel, using the same registration parameters applied to the confocal images. The final split-detector and confocal images were both montaged using commercial software (Adobe Photoshop; Adobe Systems Inc., Mountain View, CA, US).

## Results

Variable disruption of the photoreceptor bands (EZ and IZ) on OCT was observed in all seven eyes (see *Figure 1*). In all but one subject, confocal AOSLO montages showed large areas of reduced reflectivity, consistent with previously described dark areas in similar patients.[18–20] The size and location of these dark areas more closely matched the IZ disruption on OCT as opposed to the EZ disruption, consistent with previous findings examining confocal AOSLO lesions in other conditions.[18] The confocal AOSLO montage in the left panel of *Figure 2* illustrates a typical lesion observed in our subjects. The remaining MH subject (DH_10330) showed multiple focal regions of reduced reflectivity in his confocal AOSLO montage along with areas of ambiguous hyperreflectivity.

When imaged using split-detector AOSLO, numerous cone inner segments are observed within the lesion boundaries, as seen in the right panel of *Figure 2*. Using split-detector AOSLO, remnant inner segment structure was observed within the dark areas on the confocal AOSLO montages across all subjects with repaired MH or released VMT that we imaged (see *Figure 3*). Often there were patches of contiguous cone inner segments (TC_10209 (OS), PK_0858, JK_10189, DH_10244, DH_10330), while in some subjects the remnant cone population was sparsely arranged (TC_10209 (OD) and JK_10190). As cone visibility on confocal AOSLO is believed to require intact inner and outer segment structure,[21] the discrepancy between the confocal and split detection images shown here is best explained by disrupted outer segment structure in these subjects.

While cones normally appear as bright circular structures on confocal AOSLO, not all such structures are indeed derived from cones. For

## Figure 1: Spectral Domain Optical Coherence Tomography Images Obtained following Repair in Macular Hole and Vitreomacular Traction Release with Ocriplasmin

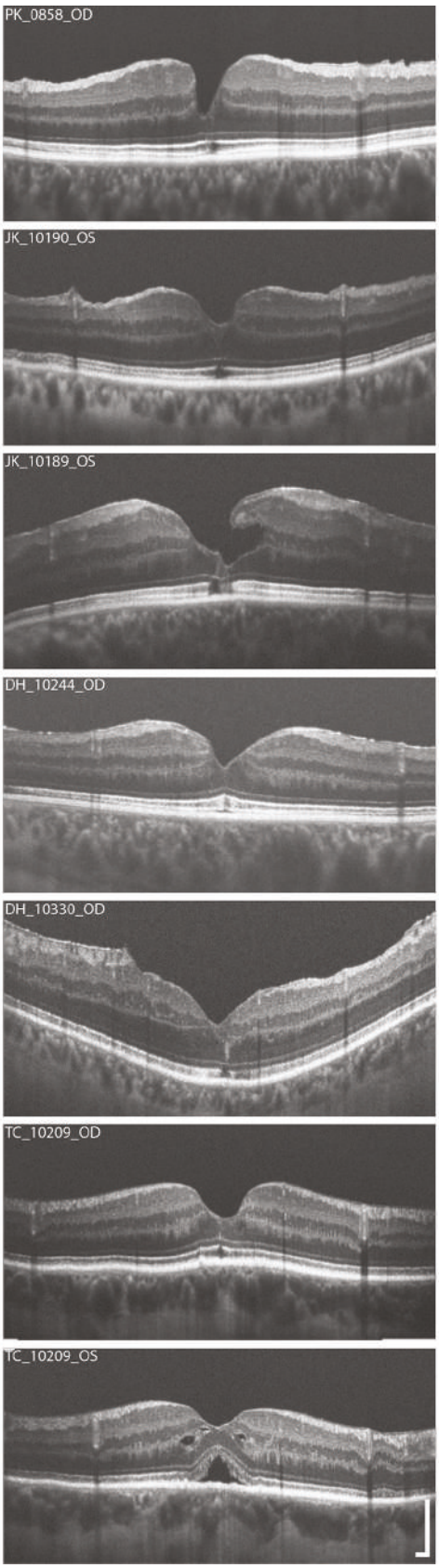


*Images were obtained just prior to adaptive optics scanning light ophthalmoscopy (AOSLO) imaging; all scans were obtained along the vertical meridian (left to right = inferior to superior). Disruptions of the interdigitation zone (IZ) and ellipsoid zone (EZ) band varying in size and severity were observed in each patient prior to AOSLO imaging despite prior surgical intervention. Scale bars = 200 µm.*

## Figure 2: Remnant Cone Structure within Confocal Adaptive Optics Scanning Light Ophthalmoscopy 'Dark Areas'

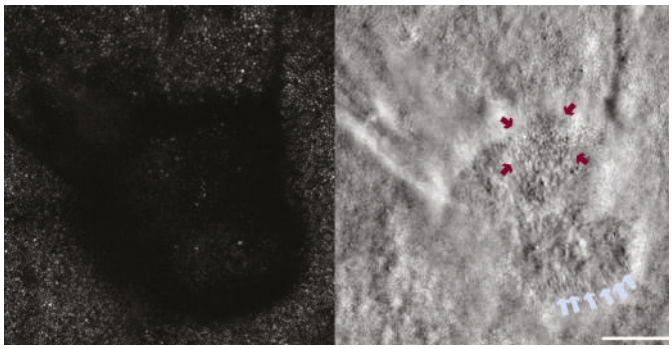

*Left, a foveal montage of a typical macular hole lesion seen with confocal adaptive optics scanning light ophthalmoscopy in subject JK_10189. Right, the corresponding lesion in the split-detection image shows inner segments within the disrupted area on confocal imagery, with a patch of contiguous inner segments near the top of the lesion (area noted by red arrows) and many presumed elongated inner segments near the lower lesion boundary (marked by blue arrows). Scale bar = 100 µm.*

## Figure 3: Comparison of Confocal and Split-detector Adaptive Optics Scanning Light Ophthalmoscopy in Macular Hole and Vitreomacular Traction Release

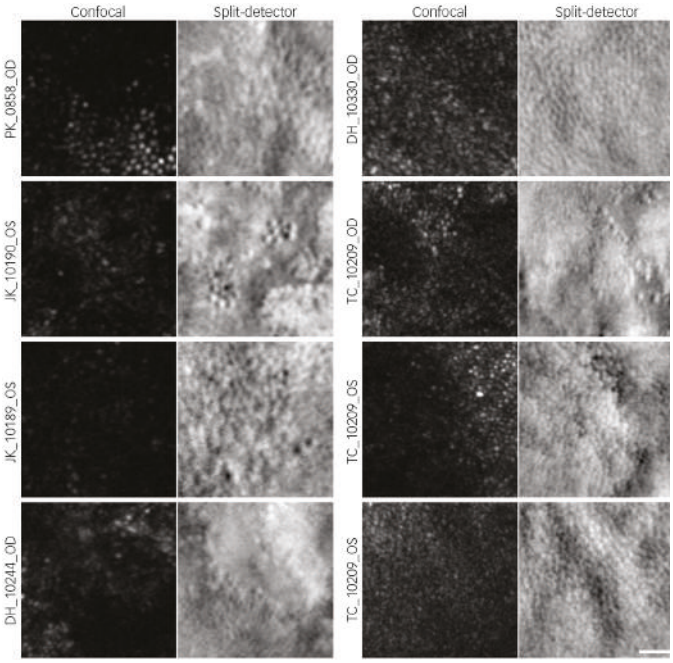


*Shown here are small regions of interest from between 100–490 µm from the fovea. Using split-detector adaptive optics scanning light ophthalmoscopy (AOSLO), remnant inner segment structure was observed across all subjects. Some showed patches of contiguous cone inner segments (TC_10209 (OS), PK_0858, JK_10189, DH_10244, DH_10330), while others had a sparse population of the remnant cone inner segments (TC_10209 (OD) and JK_10190). This remnant structure was observed despite an absence of cone reflectivity in many areas of the confocal AOSLO images. Scale bar = 20 µm.*

example, when viewed on confocal AOSLO, the RPE can produce similar-appearing structures.[24] In addition to the numerous dark areas seen in the confocal AOSLO imagery from DH_10330, we observed regions of ambiguous hyperreflectivity (see *Figure 4*) on confocal AOSLO. While some of these appeared to correspond to remnant cone inner segment structure on split-detector AOSLO (consistent with intact cones), others did not (*Figure 4*). Inspection of the OCT reveals hyperreflective material within the ONL in this subject (see *Figure 1*), which could be contributing to the granular reflective structure seen on

## Figure 4: Interpreting Hypperreflective Regions on Confocal Adaptive Optics Scanning Light Ophthalmoscopy

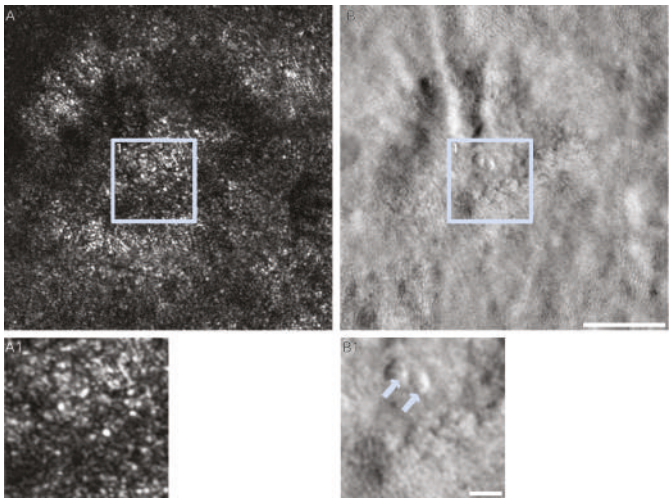


*A. A foveal montage from subject DH_10330 showing numerous circular hypperreflective structures. B. The corresponding split-detection image shows variable inner segment structure. The central area of the confocal image (A1) shows similarly sized circular structures throughout. However, when imaged using split-detector adaptive optics scanning light ophthalmoscopy (AOSLO), a contiguous array of inner segments is visible towards the bottom of B1, while the superior region shows areas absent of inner segment structure along with two larger structures of unknown origin (blue arrows). Scale bar = 100 µm (A, B) and 20 µm (A1, B1).*

the confocal AOSLO. This subject illustrates the complementary nature of OCT, confocal AOSLO and split-detector AOSLO.

## Discussion

This case series demonstrates that split-detector AOSLO can provide unique structural information in patients with history of VMT and MH. In each case, remnant inner segment cone structure was present on split-detection imagery where corresponding confocal AOSLO showed a lack of waveguiding photoreceptors. This finding directly contradicts the previous assertion that dark areas in MH lacked any photoreceptor structure.[17,19] In addition, some areas within confocal lesions containing bright reflective structures (apparent cones) did not show inner segment structure in the corresponding split detector image (DH_10330). While the split-detection channel has slightly lower resolution that could interfere with the ability to resolve the small inner segments in the central fovea, the visibility of nearby inner segments suggest these areas are truly devoid of cone structure. Together, these observations highlight the fact that not all bright circular structures within confocal AOSLO images originate from cones, and that split-detector AOSLO imaging can serve a valuable role in interpreting the degree of residual cone structure in these cases.

We previously showed that the appearance of the cone mosaic using confocal imaging can change over time in patients following MH closure, namely that cones were seen to re-emerge within the dark lesions seen initially.[18] In that study, we analysed the surrounding cone mosaic and found no significant differences across the imaging sessions, arguing against active 'migration' of nearby cones into the previously observed dark lesion.[18] Specifically, we hypothesised that the visualisation of cones in long-term follow-up imaging was due to recovery of cone outer segments within the dark lesion. A similar finding was observed in patients with macular telangiectasia, where cones become visible using confocal AOSLO in areas that appeared dark in a previous imaging session.[25] The data obtained here using split-detection AOSLO provide anatomical support for these observations, showing that inner segment structures can persist within dark lesions on confocal AOSLO. This same finding was recently reported in patients with other retinal conditions,[18,26,27] and argues for continued longitudinal examination of patients with various retinal conditions using both confocal and split-detector AOSLO.

Limitations in this study included a small sample size as well as the lens status of our subjects. Four of the eyes imaged were pseudophakic, which is a common finding due to the increased incidence in cataract development following surgical repair of MH and VMT. Pseudophakic eyes typically have poorer resolution in AOSLO imaging due to the smaller optical aperture provided by intraocular lenses. In addition, the imaging process can be difficult in patients who have lesions at their fovea; we found that most of our subjects were unable to focus reliably on the internal fixation target within the AOSLO system. To overcome this, we obtained multiple images at each intended fixation locus and returned frequently to image the fovea throughout the session, thus increasing the probability that we would have adequate retinal coverage to be able to construct a montage following image processing. However, these images are generally of lower quality than that typically achievable in phakic patients. Another limitation is the qualitative nature of the analysis. As split-detector AOSLO is quite new, there are little to no normative data with this technique and significant work remains to develop reliable analytical approaches for these new images. Nevertheless, the results shown here provide motivation for continuing to explore the complementary nature of split-detector AOSLO and conventional confocal AOSLO across other retinal conditions.

## Conclusion

Images from confocal and split-detector AOSLO are useful in identifying photoreceptor structure within lesions that are commonly observed using OCT in patients with MH and VMT. While confocal AOSLO imaging relies on intact cone waveguiding, split-detector AOSLO enables visualising cones in a manner that appears independent of their waveguide reflectivity. The results of this study imply that analyses based solely on assessment of cone structure using confocal AOSLO imagery are likely to be incorrect and should be re-evaluated. While this new imaging approach provides valuable structural insight into the repair process of MH and VMT pathology, we cannot say anything about the functional status of these cones. Moving forward, it will be important to look at results like these with tools such as AO-guided microperimetry (AOMP),[25] which overcome the inherent spatial redundancy in the stimuli employed in conventional functional assays available in the clinic. ■


1. Smiddy WE, Flynn Jr HW, Pathogenesis of macular holes and therapeutic implications, *Am J Ophthalmol*, 2004;137:525–37.
2. Smiddy WE, Michels RG, Glaser BM, deBustros S, Vitrectomy for macular traction caused by incomplete vitreous separation, *Arch Ophthalmol*, 1988;106:624–8.
3. García-Layana A, García-Arumí J, Ruiz-Moreno JM, et al., A review of current management of vitreomacular traction and macular hole, *J Ophthalmol*, 2015;2015:809640.
4. Goldberg RA, Waheed NK, Duker JS, Optical coherence tomography in the preoperative and postoperative management of macular hole and epiretinal membrane, *Br J Ophthalmol*, 2014;98(Suppl. 2):ii20–3.
5. Zhang Z, Dong F, Zhao C, et al., Natural course of vitreomacular traction syndrome observed by spectral-domain optical coherence tomography, *Can J Ophthalmol*, 2015;50:172–9.
6. Chang LK, Koizumi H, Spaide RF, Disruption of the photoreceptor inner segment-outer segment junction in eyes with macular holes, *Retina*, 2008;28:969–75.
7. Inoue M, Watanabe Y, Arakawa A, et al., Spectral-domain optical coherence tomography images of inner/outer segment junctions and macular hole surgery outcomes, *Graefes Arch Clin Exp Ophthalmol*, 2009;247:325–30.
8. Sano M, Shimoda Y, Hashimoto H, Kishi S, Restored photoreceptor outer segment and visual recovery after macular hole closure, *Am J Ophthalmol*, 2009;147:313–8.e1
9. Oh J, Smiddy WE, Flynn HW Jr, et al., Photoreceptor inner/outer segment defect imaging by spectral domain OCT and visual prognosis after macular hole surgery, *Invest Ophth Vis Sci*, 2010;51:1651–8.
10. Wakabayashi T, Fujiwara M, Sakaguchi H, et al., Foveal microstructure and visual acuity in surgically closed macular holes: spectral-domain optical coherence tomographic

analysis, *Ophthalmology*, 2010;117:1815–24.
11. Ooka E, Mitamura Y, Baba T, et al., Foveal microstructure on spectral-domain optical coherence tomographic images and visual function after macular hole surgery, *Am J Ophthalmol*, 2011;152:283–90.
12. Itoh Y, Inoue M, Rii T, et al., Correlation between length of foveal cone outer segment tips line defect and visual acuity after macular hole closure, *Ophthalmology*, 2012;119:1438–46.
13. Koizumi H, Pozzoni MC, Spaide RF, Fundus autofluorescence in birdshot chorioretinopathy, *Ophthalmology*, 2008;115:e15–20.
14. Dubra A, Sulai Y, Norris JL, et al., Non-invasive imaging of the human rod photoreceptor mosaic using a confocal adaptive optics scanning ophthalmoscope, *Biomed Opt Express*, 2011;2:1864–76.
15. Rossi EA, Chung M, Dubra A, et al., Imaging retinal mosaics in the living eye, *Eye (Lond)*, 2011:1–8.
16. Flatter JA, Cooper RF, Dubow MJ, et al., Outer retinal structure after closed-globe blunt ocular trauma, *Retina*, 2014;34:2133–46.
17. Ooto S, Hangai M, Takayama K, et al., Photoreceptor damage and foveal sensitivity in surgically closed macular holes: An adaptive optics scanning laser ophthalmoscopy study, *Am J Ophthalmol*, 2012;154:174–86.
18. Hansen S, Batson S, Weinlander KM, et al., Assessing photoreceptor structure after macular hole closure, *Retin Cases Brief Rep*, 2015;9:15–20.
19. Yokota S, Ooto S, Hangai M, et al., Objective assessment of foveal cone loss ratio in surgically closed macular holes using adaptive optics scanning laser ophthalmoscopy, *PLoS One*, 2013;8:e63786.
20. Ooto S, Hangai M, Takayama K., et al., High-resolution imaging of the photoreceptor layer in epiretinal membrane using adaptive optics scanning laser ophthalmoscopy, *Ophthalmology*, 2011;118:873–81.
21. Scoles D, Sulai YN, Langlo CS, et al., *In vivo* imaging of human cone photoreceptor inner segment, *Invest Ophth Vis Sci*, 2014;55:4244–51.
22. Tanna H, Dubis AM, Ayub N, et al., Retinal imaging using commercial broadband optical coherence tomography, *Br J Ophthalmol*, 2010;94:372–76.
23. Dubra A, Harvey Z, Registration of 2D Images from Fast Scanning Ophthalmic Instruments. In: Fischer B, Dawant B, Lorenz C, *Biomedical Image Registration*, Heidelberg: Springer Berlin, 2010;60–71.
24. Duncan JL, Zhang Y, Gandhi J, et al., High-resolution imaging with adaptive optics in patients with inherited retinal degeneration, *Invest Ophth Vis Sci*, 2007;48:3283–91.
25. Wang Q, Tuten WS, Lujan BJ, et al., Adaptive optics microperimetry and OCT images show preserved function and recovery of cone visibility in macular telangiectasia type 2 retinal lesions, *Invest Ophth Vis Sci*, 2015;56:778–86.
26. Warren C, Scoles DH, Dubris A, et al., Imaging cone structure in autosomal dominant cone rod dystrophy caused by GUCY2D mutations, *Invest Ophth Vis Sci*, 2014;55:1102.
27. Stepien KE, Scoles DH, Sulai YN, et al., Variability in photoreceptor inner segment morphology in best vitelliform macular dystrophy, *Invest Ophth Vis Sci*, 2014;55:1590.